

https://doi.org/10.1093/genetics/iyad156 Advance Access Publication Date: 21 August 2023 Plant Genetics and Genomics

Genomic mechanisms and consequences of diverse postzygotic barriers between monkeyflower species

V. Alex Sotola,^{1,5} Colette S. Berg,² Matthew Samuli,² Hongfei Chen,³ Samuel J. Mantel,¹ Paul A. Beardsley,⁴ Yao-Wu Yuan,³ Andrea L. Sweigart,^{1,*} Lila Fishman^{2,*}

*Corresponding author: Division of Biological Sciences, University of Montana, 32 Campus Dr., Missoula MT 59812, USA. Email: lila.fishman@mso.umt.edu; *Corresponding author: Department of Genetics, University of Georgia, 120 E. Green Street, Athens, GA 30602, USA. Email: sweigart@uga.edu

The evolution of genomic incompatibilities causing postzygotic barriers to hybridization is a key step in species divergence. Incompatibilities take 2 general forms—structural divergence between chromosomes leading to severe hybrid sterility in F₁ hybrids and epistatic interactions between genes causing reduced fitness of hybrid gametes or zygotes (Dobzhansky-Muller incompatibilities). Despite substantial recent progress in understanding the molecular mechanisms and evolutionary origins of both types of incompatibility, how each behaves across multiple generations of hybridization remains relatively unexplored. Here, we use genetic mapping in F₂ and recombinant inbred line (RIL) hybrid populations between the phenotypically divergent but naturally hybridizing monkeyflowers Mimulus cardinalis and M. parishii to characterize the genetic basis of hybrid incompatibility and examine its changing effects over multiple generations of experimental hybridization. In F_2 s, we found severe hybrid pollen inviability (<50% reduction vs parental genotypes) and pseudolinkage caused by a reciprocal translocation between Chromosomes 6 and 7 in the parental species. RILs retained excess heterozygosity around the translocation breakpoints, which caused substantial pollen inviability when interstitial crossovers had not created compatible heterokaryotypic configurations. Strong transmission ratio distortion and interchromosomal linkage disequilibrium in both F₂s and RILs identified a novel 2-locus genic incompatibility causing sex-independent gametophytic (haploid) lethality. The latter interaction eliminated 3 of the expected 9 F2 genotypic classes via F1 gamete loss without detectable effects on the pollen number or viability of F2 double heterozygotes. Along with the mapping of numerous milder incompatibilities, these key findings illuminate the complex genetics of plant hybrid breakdown and are an important step toward understanding the genomic consequences of natural hybridization in this model system.

Keywords: hybrid incompatibility; reciprocal translocation; transmission ratio distortion; Mimulus; sterility; reproductive isolation; Plant Genetics and Genomics

Introduction

The evolution of postzygotic reproductive barriers, caused by incompatibilities between interacting genes and/or meiotic dysfunction in chromosomally divergent hybrids, is a key component of speciation (Coyne and Orr 2004; Fishman and Sweigart 2018; Coughlan and Matute 2020). Experimental hybridization of closely related species provides a window into the nature and origins of postzygotic barriers, revealing both the genetic mechanisms of genomic incompatibility and potential magnitude of barriers to gene flow upon secondary contact. The characterization of both early- and late-generation experimental hybrid populations is a particularly promising approach (Matute et al. 2020). Multigeneration approaches can capture extrinsic incompatibilities dependent on environmental context (Walter et al. 2020), replicate natural hybrid zones (Pritchard and Edmands 2012), and, under controlled growth conditions, allow comparison of early and late hybrid generations. Additional rounds of recombination

and distinct assemblages of hybrid genotypes in later generations provide increased power to detect and localize incompatibilities (Moyle and Nakazato 2008). Furthermore, comparing patterns of hybrid breakdown across experimental generations can reveal how initial selection against incompatible genotypes shapes hybrid genomes and whether genetic and chromosomal incompatibilities quickly resolve (e.g. sort to parental genotypes) after initial hybridization or are maintained as potentially costly polymorphisms.

Fitness breakdown in experimental hybrids can be characterized in 2 complementary ways: by direct measurement of fertility, viability, and other fitness metrics and by characterizing deviations from expected Mendelian allele or genotype frequencies (transmission ratio distortion—TRD). TRD is a common feature of experimental hybrid populations, and interspecific mapping populations often exhibit significant distortion across a large fraction of their chromosomes (Fishman and McIntosh 2019). In plants, TRD at individual loci has many documented sources,

¹Department of Genetics, University of Georgia, Athens, GA 30602, USA

²Division of Biological Sciences, University of Montana, Missoula, MT 59812, USA

³Department of Ecology and Evolutionary Biology, University of Connecticut, Storrs, CT 06269, USA

⁴Department of Biological Sciences, California State Polytechnic University, Pomona, CA 91768, USA

⁵Present address: Department of Biology, State University of New York at Oneonta, Oneonta, NY 13820, USA

including environmental selection (Yin et al. 2004), meiotic drive by chromosomes (Fishman and Saunders 2008), exposure of suppressed gamete killers (Koide, Ikenaga, et al. 2008), pollen competition (Fishman et al. 2008), and Dobzhansky-Muller incompatibilities that kill gametes or zygotes (Leppälä et al. 2008; Kerwin and Sweigart 2017). In some cases, strong Dobzhansky-Muller incompatibilities (e.g. gametic or gametophytic lethals) can generate both local distortion and linkage disequilibrium between physically unlinked loci if they kill a given multilocus genotypic class (Colomé-Tatché and Johannes 2016). Although differentiating among multiple mechanisms of hybrid TRD can be challenging, joint mapping of fitness traits and TRD in multiple generations increases power and precision to characterize intrinsic postzygotic barriers.

Along with genic Dobzhansky-Muller incompatibilities, chromosomal rearrangements can play important direct and indirect roles in postzygotic breakdown. Inversions often do not cause direct underdominant effects on hybrid fertility in plants (Fishman and Sweigart 2018; Huang and Rieseberg 2020; Zhang et al. 2021), but their suppression of recombination across large genomic regions in hybrids can link multiple incompatibility loci and extend their barrier effects (Noor et al. 2001; Rieseberg 2001; Livingstone and Rieseberg 2004). Reciprocal translocations tend not to be as common as inversions within species but often distinguish sister species of flowering plants (Grant 1971; Fishman et al. 2013; Ostevik et al. 2020). In contrast to inversions, translocations can directly cause meiotic dysfunction and sterility in F₁ hybrids (Stathos and Fishman 2014); with or without crossovers, segregation of paired chromosomes with reciprocal translocations often produces at least 50% unbalanced gametes (Burnham 1956). Because novel translocations should be strongly disfavored by selection until reaching >50% frequency (Lande 1984), their initial establishment and spread in diverging populations have been a long-standing puzzle in evolutionary biology. However, some plant species maintain permanent translocation heterozygosity (Golczyk et al. 2014) and/or avoid adjacent segregation, so populations segregating for translocations may rapidly shift (genetically or epigenetically) to minimize the deleterious effects of heterokaryotypy. Thus, understanding how translocations contribute to postzygotic breakdown and genomic transmission after initial hybridization (both directly and indirectly) is an important step in understanding the processes that maintain plant species barriers.

Here, we investigate the patterns and underlying mechanisms of hybrid breakdown in multiple generations of hybrids between closely related monkeyflowers [Phin Mimulus section Erythranthe, Mimulus cardinalis, and M. parishii (also known as Erythranthe cardinalis and E. parishii)]. Despite dramatic differences in floral morphology (Beardsley et al. 2003; Fishman et al. 2015; Liang et al. 2022), hummingbird-pollinated M. cardinalis and selfer M. parishii hybridize naturally and show signatures of recent introgression where their ranges overlap in southern California (Nelson, Stathos, et al. 2021). The Erythranthe group, which also includes bee-pollinated M. lewisii, has been a long-standing model for understanding speciation by pollinator shifts and other ecological factors (Hiesey et al. 1971; Bradshaw et al. 1995; Bradshaw and Schemske 2003; Angert et al. 2008) and has recently emerged as a model system for studying Asteridae floral development (Yuan et al. 2016; Yuan 2019; Liang et al. 2022). Because phylogenomic analyses reveal substantial genomic reticulation among all taxa despite rapid morphological and structural divergence (Nelson, Stathos, et al. 2021), Erythranthe is a particularly rich system for investigating the origins, maintenance, and interactions of both pre- and postzygotic species barriers.

As a platform for investigations of both postzygotic barriers (this study) and dramatic floral, life history, and vegetative divergence, we generate dense genetic linkage maps of M. parishii \times M. cardinalis F_2 and recombinant inbred line (RIL) hybrids using genome-wide double-digest restriction-site associated DNA sequencing (ddRADseq) anchored in a new M. cardinalis genome assembly (mimubase.org). Previous coarse mapping in hybrids of each focal species with M. lewisii (Fishman et al. 2013, 2015), plus genotyping of breakpoint markers in a small number of M parishii x M. cardinalis hybrids (Stathos and Fishman 2014), suggest that these naturally hybridizing taxa are distinguished by at least one reciprocal translocation. High-resolution genomewide mapping of male fertility (pollen viability and number) and TRD in each generation allows us to address specific hypotheses about putative barriers, identify major genic and chromosomal incompatibilities genome-wide, and track their evolution and influence from F2 to advanced-generation hybrids.

Specifically, we ask: are patterns of postzygotic breakdown (hybrid sterility and TRD) consistent in multiple environments (i.e. between different F₂ populations) and through multiple generations of self-fertilization (F2 hybrids vs RILs)? In particular, are epistatic genic incompatibilities causing hybrid sterility rapidly lost during RIL construction, resulting in restored fertility but loss of incompatible genotypic combinations? Do chromosomes with reciprocal translocation sort to parental or other meiotically compatible karyotypes in advanced-generation hybrids, or does chromosomal underdominance persist? Does TRD and crosschromosome linkage disequilibrium due to other sources dissipate (as might be the case with some postmating prezygotic barriers such as pollen competition) or amplify (as might occur with some recessive incompatibilities or directional selection) with multiple generations of selfing? Are major incompatibility loci shared with other Mimulus section Erythranthe hybrids, or are there novel postmating reproductive barriers unique to this florally divergent cross?

Methods

Study system and plant lines

The monkeyflowers of the M. cardinalis species complex (Mimulus section Erythranthe; Phrymaceae) are a well-established model system for understanding the genetics of floral evolution and speciation (Yuan 2019). Hummingbird-pollinated M. cardinalis has a broad latitudinal range in the western United States with distinct Arizonan, Southern Californian, and Sierran clades (Nelson, Stathos, et al. 2021). M. cardinalis is parapatric in the Sierras with bee-pollinated high-elevation specialist M. lewisii, where reproductive isolation is maintained by local adaptation to divergent habitats and pollinator preferences (Hiesey et al. 1971; Bradshaw and Schemske 2003; Ramsey et al. 2003), as well as 2 reciprocal translocations causing underdominant F1 hybrid sterility (Fishman et al. 2013; Stathos and Fishman 2014). M. parishii is a small-flowered annual selfer restricted to Southern California, where it cooccurs with M. cardinalis in ephemerally wet desert washes. Hybrids between M. cardinalis and M. parishii have been observed in the field, and local sharing of identical organellar genomes (as well as nuclear reticulation) indicates an extensive history of mating and introgression despite extreme differences in floral morphology (Nelson, Stathos, et al. 2021).

The plants in this study were all derived from 2 highly (>10 generations) inbred lines of Sierran M. cardinalis (CE10) and M. parishii (PAR), which were also used in previous investigations of species barriers (Bradshaw et al. 1998; Schemske and Bradshaw 1999; Bradshaw and Schemske 2003; Ramsey et al. 2003; Fishman et al. 2013, 2015; Nelson, Muir et al. 2021). We generated PAR \times CE10 F_1 hybrids by hand-pollination (with prior emasculation of the PAR seed parent in the bud) and F2 hybrids by self-pollination of F1 hybrids. The F2 hybrids were grown in 2 separate greenhouse common gardens at the University of Montana (UM- F_2 ; total N = 524) and the University of Connecticut (UC- F_2 N = 253), along with parental control lines, and were phenotyped for numerous floral and vegetative traits including the pollen fertility traits presented here. RILs were generated by single-seed-descent from additional F₂ individuals grown at the University of Georgia and California State Polytechnic University, Pomona; a total of 167 RILs were formed through 3-6 generations of self-fertilization.

DNA extraction and sequencing

Genomic DNA was extracted from bud and leaf tissue of the greenhouse-grown F2 and RIL mapping populations using a cetyltrimethylammonium bromide (CTAB) and chloroform protocol modified for 96-well plates (dx.doi.org/10.17504/protocols.io.bgv6jw9e). We used a ddRADSeq protocol to generate genomewide sequence clusters (tags), following the BestRAD library preparation protocol (dx.doi.org/10.17504/protocols.io.6awhafe), using restriction enzymes PstI and BfaI (New England Biolabs, Ipswich, MA, USA). Postdigestion, half plates of individual DNAs were labeled by ligation of 48 unique in-line barcoded adapters and then pooled for size selection. Libraries were prepared using NEBNext Ultra II library preparation kits for Illumina (New England BioLabs). Each pool was indexed with a unique NEBNext i7 adapter and an i5 adapter containing a degenerate barcode and PCR amplified with 12 cycles. The F2 libraries were size-selected to 200-700 bp using BluePippin 2% agarose cassettes (Sage Science, Beverly, MA, USA) and sequenced (150-bp paired-end reads) in a partial lane of an Illumina HiSeq4000 sequencer at GC3F, the University of Oregon Genomics Core Facility. The RIL library was sequenced (150-bp paired-ends) without size-selection on an Illumina HiSeq4000 at Genewiz (South Plainfield, NJ, USA).

Sequence processing and linkage mapping

After sequencing, two separate ddRAD data sets were analyzed: one with samples from both F_2 populations (N = 283 UM- F_2 hybrids with 3 M. parishii and 2 M. cardinalis controls, and 253 UC-F₂ hybrids, with 3 each F₁, M. parishii and M. cardinalis controls) and one with samples from the RIL population (N = 167). Samples from both data sets were demultiplexed using a custom Python script (dx.doi.org/10.17504/protocols.io.bjnbkman), trimmed using Trimmomatic (Bolger et al. 2014), mapped to the M. cardinalis CE10 v2.0 reference genome (http://mimubase.org/FTP/ Genomes/CE10g_v2.0) using the Burrows-Wheeler Aligner maximal exact match (bwa-mem) algorithm and indexed using SAMtools (Li et al. 2009). The RIL data set was also filtered in SAMtools using a mapping quality ≥29. We called SNPs in both data sets using HaplotypeCaller in GATK v3.3 in F₂s, v4.1.8.1 in RILs (McKenna et al. 2010).

Next, we performed a series of filtering steps to generate sets of high-quality SNPs. In the F2 dataset, we filtered using vcftools (Danecek et al. 2011), retaining sites with read depth ≥5, mapping quality ≥10, and <40% missing data. We also filtered out loci deviating from Hardy–Weinberg Equilibrium at P < 0.00005; this threshold was empirically chosen to only remove rare clusters of "bad" SNPs (generally entire tags with high excess heterozygosity due to crossmapping of reads) deviating strongly from the overall trends in transmission distortion across chromosomes (Supplementary Fig. 1). In the RIL data set, we filtered a combined GVCF file using default quality control parameters in GATK, retaining sites with read depth $\geq 4 \times N$ (with N = number of RIL samples) and

<10% missing genotypes. For both data sets, we used custom scripts to remove sites that were not polymorphic in the parents and heterozygous in the F₁ hybrids (F₂: https://github.com/bergcolette/F2_ genotype_processing). We excluded individuals from the F2 data set with >10% missing data and from the RIL dataset with low coverage, high missingness, or excessive heterozygosity (>50%, indicating line contamination). These filtering steps produced an F2 data set with 18,119 SNPs (N = 252 UM- F_2 and 253 UC- F_2) and an RIL data set with 47,851 SNPs (N = 145).

To produce sets of high-quality marker genotypes for mapping, we binned each data set into 18-SNP windows using custom Python and R scripts (provided at github links above), requiring ≥8 sites to have SNP genotype calls to assign a windowed genotype. In the F₂ binning script, M. cardinalis homozygotes were coded as 2, M. parishii homozygotes as 0, and heterozygotes as 1. We called windows with mean values < 0.2 as parishii homozygotes, >1.8 as cardinalis homozygotes, and between 0.8 and 1.2 as heterozygotes. Windows with means outside of these ranges were coded as missing genotypes. For the RILs, we required ≥88% of SNP calls to match each other to assign the window homozygous genotype (e.g. 16/18 sites must be called M. parishii homozygotes to assign that window as M. parishii; the same is true for heterozygotes and M. cardinalis homozygotes; https:// github.com/vasotola/GenomicsScripts).

We generated linkage maps for each data set using Lep-MAP3 (Rastas 2017). First, we used the SeparateChromosomes2 module to assign markers to linkage groups (F_2 : LodLimit = 25, theta = 3, RIL: LodLimit = 28, theta = 0.2). In the RIL data set, 10 markers were assigned to linkage groups inconsistent with the reference genome assembly; we manually reassigned these markers to linkage groups corresponding to their reference assembly chromosomes. Next, we performed iterative ordering using the OrderMarkers2 module (Kosambi mapping function; 6 iterations/ per linkage group in the F2s, 10 in the RILs); the order with the highest likelihood for each linkage group was chosen. This resulted in an F₂ map with 997 markers in 7 linkage groups and an RIL map with 2,535 markers in 8 linkage groups. In the RIL data set, the genotype matrix output by Lep-MAP3 differed in 2 important respects from the input file. First, due to stringent thresholds for calling windowed genotypes, our input file includes a high percentage of missing data (23% of genotypes are coded as "no call"), whereas the output file contains no missing data (Lep-MAP3 converts each "no call" genotype to a called genotype). Second, the Lep-MAP3 output file contains more heterozygous genotype calls than the input file. The reason for this increase in heterozygosity is that Lep-MAP3 disproportionately converts "no call" genotypes to heterozygotes: relative to the input file, the output genotype matrix includes 115% more heterozygotes, compared to only 18% more M. cardinalis homozygotes and 20% more M. parishii homozygotes. Notably, Lep-MAP3 frequently converted "no call" genotypes to heterozygotes when they occur at single markers between recombination breakpoints. Because most recombinational switches in this RIL population are between alternative homozygotes, any window that contains an actual breakpoint will carry a mixture of M. cardinalis and M. parishii homozygotes at the 18 SNPs (and thus be coded as "no call" in our windowed genotype matrix). To circumvent these problems, for all downstream analyses, we used a modified version of the genotype matrix output from Lep-MAP3 in which genotypes were recoded as "no call" as in the input file.

TRD and linkage disequilibrium

Genotype frequencies were calculated, plotted, and tested for significant deviation from Mendelian expectations (X² with 2 df) separately for the 2 F₂ populations. TRD due solely to extrinsic factors (e.g. selection on parental alleles affecting germination under different conditions, environmentally dependent hybrid incompatibilities) may be distinct between the F2 growouts (Fishman and McIntosh 2019), whereas TRD due to intrinsic genic or chromosomal incompatibilities may be more likely to be shared. For the RILs, we conducted parallel tests with expectations for alternate homozygotes set to 0.47 and heterozygotes to 0.06, which is the expectation given our final composition of RILs (9 individuals with 3 generations of selfing, 116 with 4, 19 with 5, and 1 individual with 6 generations of selfing). For all sets, we used both uncorrected (a = 0.01; critical value = 6.635) and stringent (Bonferonni-corrected; F₂ critical value = 16.442, RIL critical value = 18.217) chi-squared tests to assess the significance of distortion.

We used the package pegas (Paradis 2010) in the program R (R Core Team 2021) to calculate pairwise linkage disequilibrium (r) between all markers within the UM-F2 and RIL mapping populations. To minimize false positives driven by the large number of pairwise comparisons, we plotted only those r values greater than the 95% quantile after bootstrapping 1,000 times. All plots were visualized with R.

QTL mapping of pollen traits

In the UM-F2 and RIL populations, we directly assessed male fertility by collecting all 4 anthers of the first flower from each plant into 50 mL of lactophenol-aniline blue dye. We counted viable (darkly stained) and inviable (unstained) pollen grains using a hemocytometer (≥100 grains/flower). We estimated total pollen grains per flower (count per mL \times 50) and pollen viability as viable grains/total counted. For a handful of individuals with <100 pollen grains counted, pollen viability was scored as missing data. Phenotyping in the RIL population was performed on siblings or selfed progeny of the individuals genotyped. In a few cases in the RILs (N = 12), the first flower had <100 pollen grains, so both traits were instead collected from the second flower.

We mapped pollen quantitative trait loci (QTLs) in Windows QTL Cartographer 2.5 (Wang et al. 2012) using composite interval mapping (CIM; Zeng 1993, 1994), with forward-backward stepwise regression, a window size of 10 cM, 5 background markers, and a 1-cM walk speed. We used permutations (N = 1000) to set genomewide significance thresholds for QTL peaks and calculated 1.5-LOD drops to determine confidence intervals for QTL locations. Because pollen viability QTLs exhibited complex interactions in F2s (see Results), we directly estimated QTL effects (at each peak marker) and interactions using the Generalized Linear Model module in JMP16 (SAS Institute, Cary, NC, USA, starting with a full factorial model of all QTLs and two-way interactions and removing nonsignificant (P > 0.05) interactions. To test for pollen viability signatures of a 2-locus gametic incompatibility (LG4-LG8) detected from TRD and linkage disequilibrium (LD) patterns, we contrasted Least Squared Means for each extant F2 class from an ANOVA also including the large-effect translocation breakpoint marker at 60.55 Mb on Chr 6.

QTL mapping of underdominant effects in RILs has low power due to (relatively) few heterozygotes, plus most RIL QTL-mapping algorithms (including those in WinQTLCart) exclude nonhomozygous genotypes. To directly test for persistent underdominant effects of the Chr 6–7 translocation in RILs, we screened for genotype-pollen viability associations at uniquely positioned markers with a joint sample size >70 across the breakpoint region (57.07-61.08 Mb of Chr6 and 7.51–13.05 of Chr 7; n = 42), using t-tests in the response screening module in JMP16 (SAS Institute, Cary, NC, USA). However, we caution that because RIL hybrid male sterility was measured on siblings or descendants of the genotyped individuals, underdominant effects will likely be underestimated. That is, regions genotyped as heterozygous might actually be homozygous in phenotyped individuals, potentially explaining why a few of them are highly fertile. We conservatively controlled for multiple tests by using an false discovery rate (FDR)-corrected P-value of 0.05.

Results

Comparative linkage mapping

Across most of the genome, the F2 and RIL genetic maps are highly collinear, with linkage groups and marker order largely reconstructing the physical order of the 8 chromosomes of the M. cardinalis reference genome (Supplementary Figs. 2 and 3). The notable exception to this pattern involves markers on Chromosomes (Chr) 6 and 7, where previous work suggested an M. cardinalis-specific reciprocal translocation vs both M. parishii and M. lewisii (Fishman et al. 2013, 2015; Stathos and Fishman 2014). There is no single linear order of markers in heterozygotes for a reciprocal translocation (Livingstone et al. 2000), which generates linkage across the entire involved chromosomes during F₁ meiosis and a continuous LG 6&7 in the F2 hybrids. In the RILs, the portion of Chr 6 distal to the translocation forms a distinct linkage group, while tight linkage between markers on the end of Chr 6 and the first 8 Mb of Chr 7 in M. cardinalis (purple and green/red segments, respectively, in Fig. 1) generates a second composite linkage group. The RIL map is \sim 35% longer than the F_2 map (total length = 892.95 vs 661.37 cM), consistent with the additional generations of recombination. In both maps, recombination rates per Mb are dramatically lower (near zero) across the central 20-40 Mb of each chromosome (Supplementary Fig. 2). This pattern is also evident for all chromosomes other than Chr 7 in an intraspecific M. cardinalis map (Nelson, Muir, et al. 2021; Nelson, Stathos, et al. 2021), consistent with a primarily metacentric chromosomal structure in Erythranthe species.

Genome-wide patterns of TRD

All linkage groups, with the exception of LG2 in the UM-F₂ mapping population, exhibited strong TRD in all 3 maps (Fig. 2; Supplementary Fig. 4, Supplementary Tables 2 and 3). Patterns of TRD were very similar between the 2 F2 populations, suggesting that TRD primarily reflects shared aspects of the hybrid context (e.g. pollen competition or incompatibilities) vs local environmental selection (e.g. germination conditions different between the 2 growouts). The 2 F2 growouts shared regions of excess M. cardinalis homozygosity on LGs 1, 4, 5, and 6 (distal to translocation), excess M. parishii on LG8, and excess heterozygosity on LG3 and in the translocation region on LG6&7. The UC-F2 also exhibited excess heterozygosity and M. cardinalis alleles on LG2. Additional generations of recombination and selection in the RIL population strengthened and refined the locations of shared TRD peaks on LGs 1, 2, 3, 6&7, and 8. However, RILs exhibited a novel region of very strong M. parishii excess on one arm of LG5; this signal was absent or opposite in the F2 hybrids, suggesting an advantage of M. parishii alleles in this region specific to either the environment or the increasingly homozygous genetic background of RIL formation. In addition to local peaks of TRD, the RIL population exhibited slightly higher residual heterozygosity across the genome (9.3%) than the Mendelian expectation [6% (Fig. 2)]. While some of this overall excess is due to major local peaks in heterozygosity shared with the F₂ hybrids (e.g. on LG3 and in the LG6&7 breakpoint region, Fig. 2), the remainder may reflect genome-wide

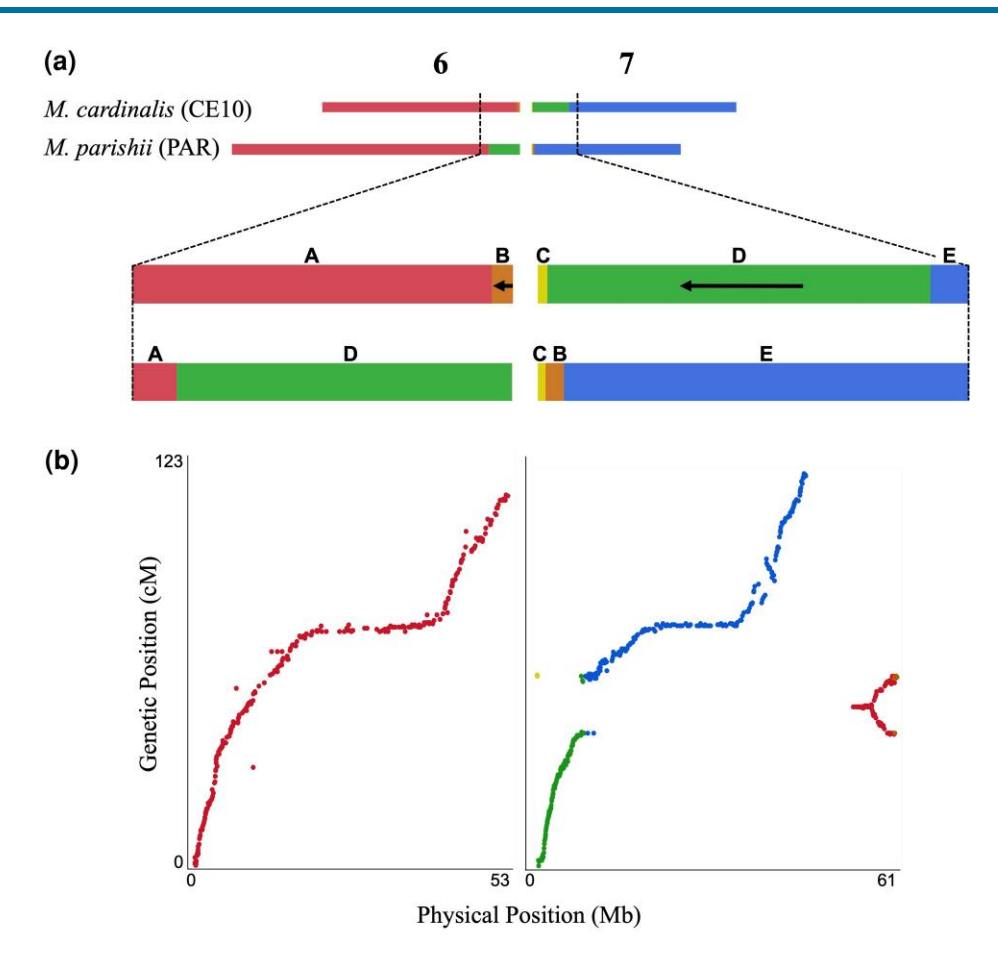


Fig. 1. Mimulus cardinalis (CE10) and M. parishii (PAR) exhibit a reciprocal translocation between Chromosomes (Chr) 6 and 7. a) Schematic showing the affected chromosomes and regions with the CE10 order labeled A to E from left to right: a distal region of Chr 6 in PAR has moved to Chr 7 in CE10 (segment D) and a smaller region of Chr 7 in PAR has moved to the end of Chr 6 in CE10 (segment B). Black arrows indicate blocks where the CE10 order is inverted relative to the ancestral PAR order. Genome coordinates for the blocks are given in Table S1. b) Plot of physical position (Mb, CE10g_v2.0) by genetic position for RIL linkage groups (LGs) 6 and 6&7. SNP markers (dots) are colored by the locations defined in (a). RIL LG6 includes only markers from the collinear region of Chr 6. RIL LG6&7 includes all markers from the translocated regions, but the genetic order reflects multiple distinct linkages associated with the divergent parental chromosomes (e.g., markers near the translocation breakpoint at ~60 Mb in CE10 are tightly linked to markers in all other segments).

selection against weakly incompatible parental homozygous combinations in the RILs (Thompson et al. 2022).

Tests of hybrid incompatibilities as the source of TRD

To investigate whether peaks of TRD were caused by hybrid incompatibilities (e.g. gametic or zygotic lethals), we characterized pairwise LD between all markers in the UM-F₂ and RIL populations (Fig. 3; Supplementary Tables 4 and 5). In the F₂ hybrids, there was significant off-diagonal LD over most of LG6 and 7 (due to the translocation), between LG4 and the center of LG8, and between the distal ends of LG2 and LG8. In the RILs, parallel TRD on different chromosomes (e.g. near fixation of M. parishii alleles on both LG5 and LG8) can cause high interchromosome LD even without epistatic selection during RIL formation. Thus, it is not surprising that, in addition to sharing the F2 LD regions, the RILs exhibit more abundant and diffuse LD genome-wide (Fig. 2, Supplementary Table 5). However, some of these regions may house multilocus incompatibilities that are too mild and/or late-acting to be statistically detected in the F2 generation (e.g. F2 sporophytic hybrid sterility).

Strong and opposite TRD on LG4 (excess M. cardinalis) and LG8 (excess M. parishii) in the F2 hybrids (Fig. 2), as well as high and persistent LD between these regions (Fig. 3), suggested a major 2-locus incompatibility. To investigate further, we tallied all 2-locus genotype combinations at TRD-peak markers (6.8 Mb on Chr 4, 40 Mb on Chr 8; Fig. 2; Supplementary Fig. 4) in both the UM-F₂ and RIL populations (Table 1). These regions clearly deviate from the Mendelian expectation of independent segregation, with 3 of the expected 9 genotypic classes entirely absent from both populations (Table 1). To test for the mechanism, we calculated the expected genotype frequencies under 2 different scenarios: (1) a gametic incompatibility in which all haploid gametes (both pollen and ovules) are inviable if they carry the M. parishii-M. cardinalis allelic combination at LG4 and LG8 (i.e. P;C gametes missing), and (2) a 2-locus dominant zygotic incompatibility in which hybrids die if they carry at least one M. parishii allele at LG4 and at least one M. cardinalis allele at LG8 (P_; C_ zygotes die). In the F₂ population, genotype frequencies best fit the sexindependent gametic incompatibility model, which distinctively predicts the numerous double heterozygotes observed (Table 1). The RIL genotypes are also most consistent with a sexindependent gametophytic mechanism; however, the observed

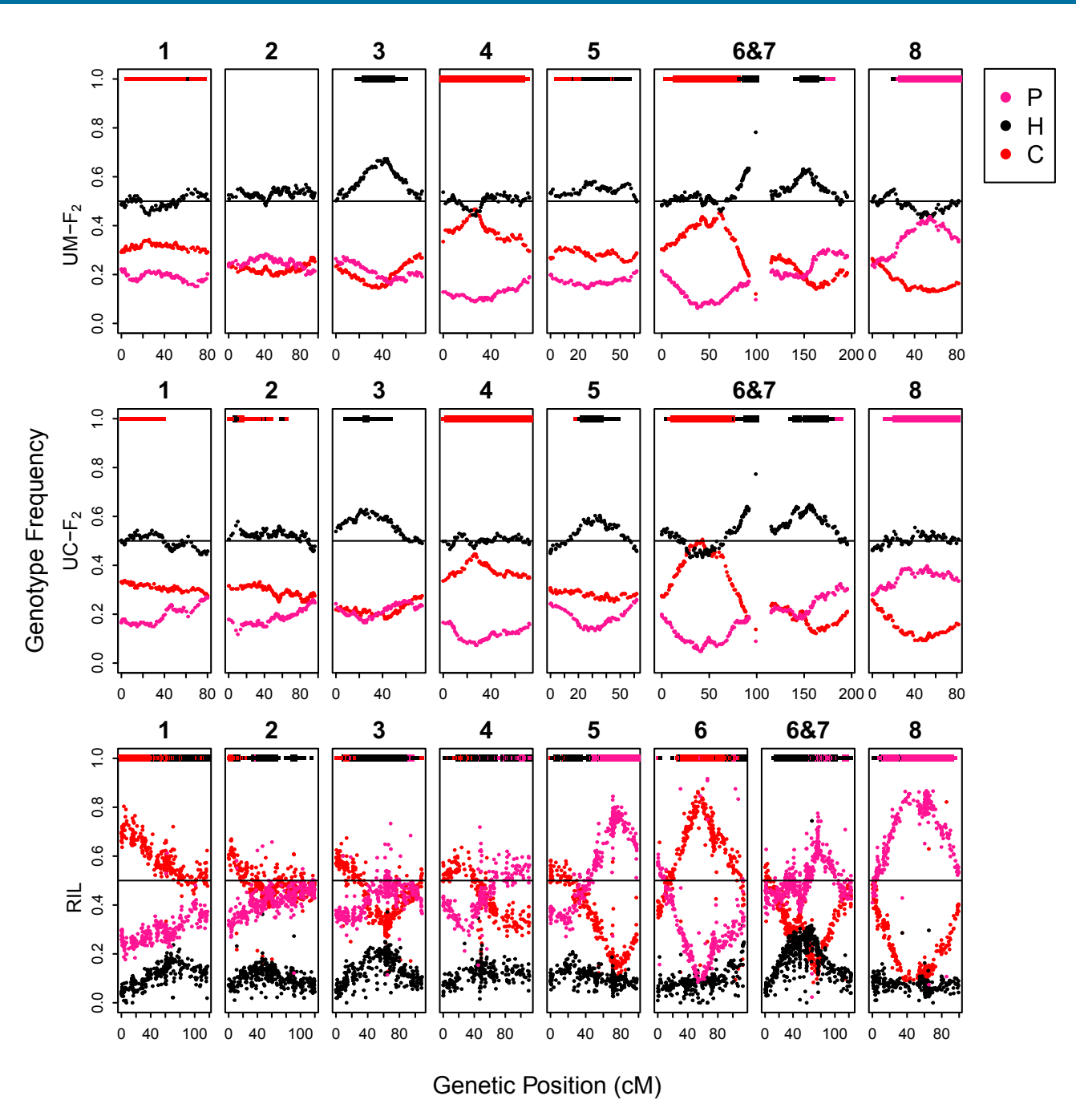


Fig. 2. Genotype frequencies across each linkage group in the F2 and RIL populations. Red dots indicate homozygous M. cardinalis, pink is homozygous M. parishii, and black is heterozygous. The bars at the top of each plot indicate regions with significant transmission ratio distortion by X^2 tests at $\alpha = 0.01$ (thin lines, critical value = 6.635) and at a more stringent, Bonferonni-corrected level (thick lines, F2 critical value = 16.442, RIL critical value = 18.217).

excess of M. parishii transmission on LG8 exceeds that expected from a gametic incompatibility alone.

Genetics of male fertility traits in hybrids

F₂ Hybrids (UM-F₂) exhibited substantial variation for pollen viability (mean = 0.48, but significantly nonnormal by Shapiro-Wilks test, P < 0.0001; Supplementary Fig. 5), whereas both parental lines were relatively fertile (mean = 0.73 for CE10 and 0.84 for PAR, N = 2and 8, respectively). A major underdominant pollen viability QTL mapped to the translocation breakpoints on LG6&7, along with smaller QTLs on LGs 2, 3, and 4 (Fig. 4; Table 2). To investigate the contribution of epistasis to the observed pollen inviability and test for unlinked modifiers of the translocation-associated underdominant sterility, we conducted a model selection analysis starting with a factorial model of the 4 peak markers and all 2-way interactions. Only interactions including LG6&7 were significant at P = 0.05(along with all 4 single QTLs), so we interpret QTL effects under that reduced model ($r^2 = 0.42$). The LG6&7 QTL was strongly underdominant (Table 2), while the other 3 pollen viability loci exhibited at least partial dominance of the M. parishii allele, with M. cardinalis homozygotes significantly more fertile than heterozygotes and M. parishii on LG4, significantly less fertile on LG3, and heterozygotes most fertile

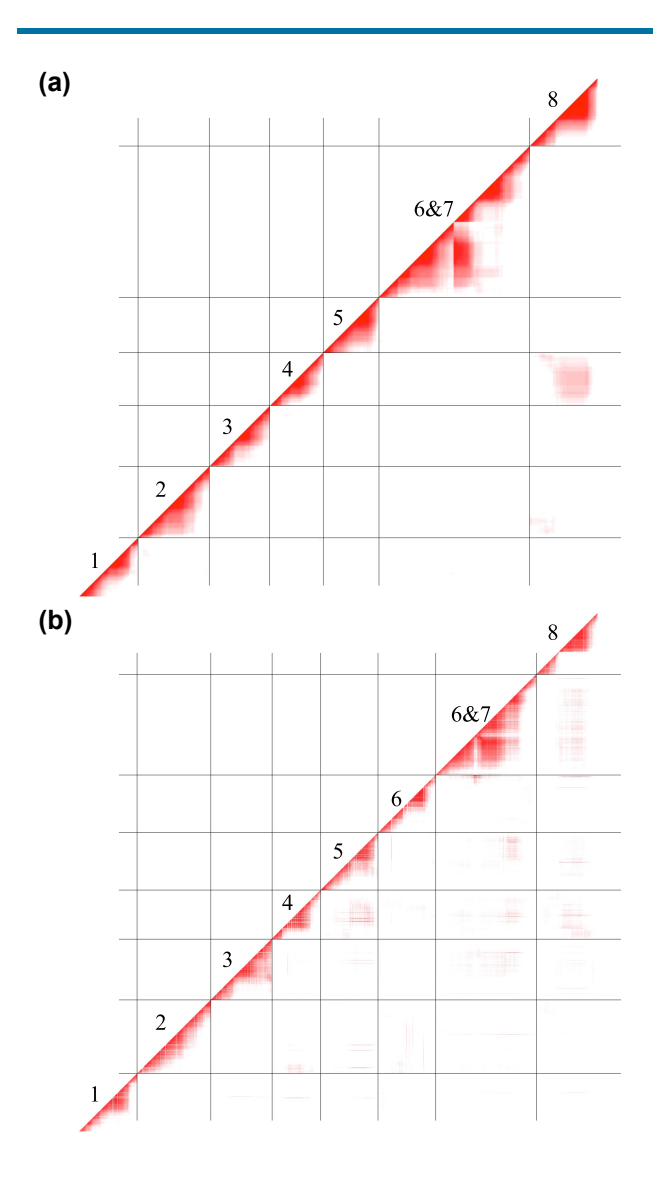


Fig. 3. Linkage disequilibrium heatmaps for M. parishii x M. cardinalis UM-F2 a) and RIL b) populations, ordered by linkage group. Data shown are r values greater than the 95% quantile after bootstrapping (95% F2: 0.176; 95% RIL: 0.305). Values range from 0 (white) to 1 (dark).

(but not significantly different from M. cardinalis) on LG2. The interactions involving the QTL on LG6&7 did not appear to modify the low fertility of translocation heterozygotes, which was consistent across genetic backgrounds (i.e. LG6&7 heterozygotes with alternative genotypes elsewhere were indistinguishable by Tukey's Honest Significant Difference tests; Supplementary Fig. 6). Instead, the interactions involved idiosyncratic combinations of other genotypes, generally with low sample sizes; for example, F2 hybrids with M. parishii genotype at QTL PV3 and M. cardinalis at PV6&7 were about twice as fertile [least squared mean (LSM) = 0.86 ± 0.11 , N = 2] as those with the opposite homozygous combination (LSM = $0.45 \pm$ 0.06, N = 8).

The RILs were, on average, highly fertile compared to the F2 hybrids (mean pollen viability = 0.76; Supplementary Fig. 5), and we detected no significant RIL pollen viability QTLs in WinQTLCart (Supplementary Fig. 7). However, marker genotypes across the translocation region exhibited significant associations with pollen viability (26/42 significant at uncorrected P<0.05, 18/42 at FDR-corrected P < 0.05). For example, at the peak marker close

to the Chr7 breakpoint (Chr7_10.47), heterozygotes were ~25% less pollen-fertile, on average, than the parental genotypes (H: 0.64 ± 0.04 , n = 18; $C = 0.79 \pm 0.04$, n = 18, $P = 0.79 \pm 0.03$, n = 32). Markers on Chr6 showed parallel patterns, though they showed less distortion against M. cardinalis homozygotes. Although some RILs genotyped as heterozygous for LG6&7 markers were highly fertile, consistent with segregation to homozygosity between the genotyped and phenotyped generation (see Methods) and/or stabilization of compatible chromosomal configurations, the underdominant fertility effects of the translocation persist.

Consistent with the parental species' difference in mating system, pollen number in the UM-F2 experiment was nearly seven-fold higher in M. cardinalis than in M. parishii, though the sample size was too small to confirm this statistically (mean pollen number: $CE10 = 50.38 \times 10^3$, N = 2; $PAR = 7.62 \times 10^3$, N = 8). Pollen number in the F2 hybrids was intermediate (mean =38.94 \times 10³, N = 245; Supplementary Fig. 5), and we mapped 3 QTLs that together explain only \sim 20% of the F₂ variance (Fig. 4; Table 2), consistent with a polygenic basis to quantitative divergence in pollen production. For 2 of the 3 F₂ QTLs, M. parishii homozygotes had the lowest pollen counts, while the other (on LG6&7) appeared overdominant (heterozygotes producing most pollen), and there were no significant interactions among QTLs in pairwise tests In the RIL grow-out, pollen counts were overall higher but followed the same pattern, with M. cardinalis ~7x as pollenproductive and hybrids generally intermediate (mean pollen number: RILs = 19.02×10^3 , N = 100; CE10 = 32.26×10^3 N = 17; PAR = 4.39×10^3 , N = 11; Supplementary Fig. 5). QTLs on LG1 and LG6 together explain ~48% of the RIL variance in pollen production, with M. parishii homozygotes at each producing less pollen and no evidence of interactions (Table 2; Supplementary Fig. 7). The genetic bases of variation in pollen number and viability were largely independent, with no significant phenotypic correlation and, with the exception of the region of suppressed recombination near translocation breakpoints, no QTL coincidence in the F₂ hybrids (Table 2; Fig. 4).

Notably, F2 pollen viability (or pollen number) QTLs cannot account for the LG4-LG8 gametic incompatibility. Although the LG4 pollen viability QTL is coincident with the LG4 gametic incompatibility locus at ~6.8 Mb, individuals carrying at least one M. parishii allele have reduced pollen viability regardless of their LG8 genotype, producing a M. parishii-dominant effect (Table 2; Supplementary Fig. 6b). Due to the lack of F₁-recombinant P;C gametes (and P;C, H:C, and P;H F₂s), the H;H F₂ class is the only one capable of forming the incompatible gamete combination (i.e. one-fourth should be missing or sterile). Instead, P;P individuals (all gametes compatible) were just as male-fertile (mean pollen viability = 0.48 ± 0.03 SE, N = 24) as the H:H class (mean = $0.49 \pm$ 0.02, N = 53), consistent with an alternative cause.

Discussion

M. parishii × M. cardinalis genetic maps and RILs: a resource for understanding extreme floral divergence and speciation

The monkeyflowers of Mimulus section Erythranthe have been a model system for understanding plant speciation for over 5 decades, with a primary focus on the floral and elevational adaptation of parapatric M. lewisii and M. cardinalis. Here, we develop foundational genetic maps and RIL resources for the far more florally divergent, yet sympatric and hybridizing, pair of M. parishii and M. cardinalis. Despite structural divergence and substantial hybrid incompatibilities, we constructed consistent and high-quality

Table 1. Two-locus segregation pattern for loci on LG4 (6.75–7.65 Mb) and LG8 (12.87–40.08 Mb) showing opposite single-locus TRD and strong LD in M. parishii × M. cardinalis F₂ hybrids and RILs.

| | UM-F ₂ population | | | | RIL population | | | | |
|-----------------------|------------------------------|-----------|-------------------------|---------------------------|----------------|-----------|-------------------------|---------------------------|--|
| Genotype (LG4;LG8) | Observed | Mendelian | P;C gametes inviable | P_;C_ zygotes inviable | Observed | Mendelian | P;C gametes inviable | P_;C_ zygotes inviable | |
| C;C | 24 | 16 | 29 | 37 | 18 | 31 | 42 | 42 | |
| H;C | 0 | 32 | 0 | 0 | 0 | 2 | 0 | 0 | |
| P;C | 0 | 16 | 0 | 0 | 0 | 31 | 0 | 0 | |
| C;H | 61 | 32 | 57 | 73 | 6 | 2 | 4 | 6 | |
| H;H | 53 | 64 | 57 | 0 | 6 | 4 | 4 | 0 | |
| P;H | 0 | 32 | 0 | 0 | 0 | 2 | 0 | 0 | |
| C;P | 27 | 16 | 29 | 37 | 40 | 31 | 42 | 42 | |
| H;P | 58 | 32 | 57 | 73 | 21 | 2 | 4 | 6 | |
| P;P | 34 | 16 | 29 | 37 | 47 | 31 | 42 | 42 | |

For each population, observed counts of individuals with each of the 9 possible genotypes (C = M. cardinalis homozygote, P = M. parishii homozygote, and H = heterozygote) are compared with expected counts under normal Mendelian inheritance (Mendelian), expected counts under a model of sex-independent gametic inviability (P;C gametes inviable), and expected counts under a model of dominant zygote inviability (P;C_ zygotes inviable). Counts are shown rounded to the nearest integer. See Supplementary Table 6 for unrounded counts and frequencies.

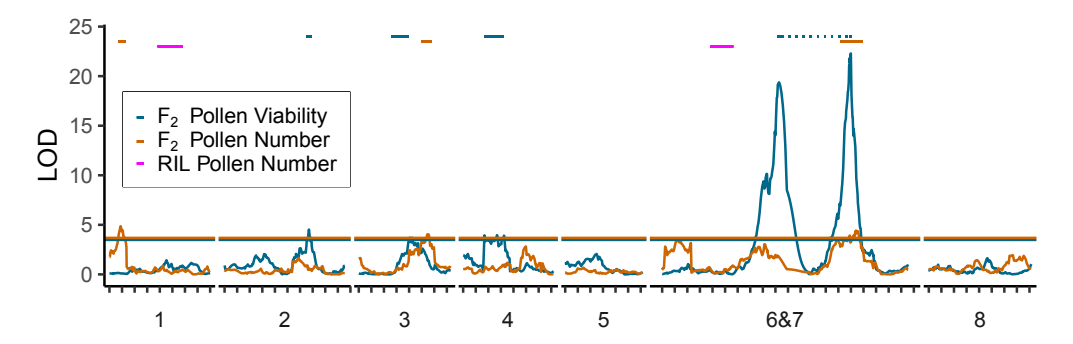


Fig. 4. QTLs for pollen viability (blue) and pollen number (orange) in M. $parishii \times M$. $cardinalis F_2$ hybrids, as well as the locations of 2 pollen number QTLs in descendant RILs (pink, aligned by the physical position of markers). Horizontal lines denote the permutation-derived (N = 1000) LOD significance thresholds for each F_2 trait, and the bars indicate QTL confidence intervals (1.5 LOD drop). The single major underdominant pollen viability QTL associated with the LG6&7 translocation maps to markers near both breakpoints (QTL locations connected by light dotted line), which cannot be linearly resolved in F_2 hybrids. Because the RIL QTL-mapping algorithm excluded heterozygotes, no RIL pollen viability QTLs were detected despite the negative effects of retained heterozygosity (see text).

ddRAD-based genetic maps to guide future investigations of the genetic and molecular mechanisms of floral, mating system, and life history evolution. Previous genetic maps in the Erythranthe group have used sparse PCR-based (Bradshaw et al. 1998; Fishman et al. 2013, 2015) or targeted capture markers; successful extension of this high-density gene-centric ddRAD genotyping technique from M. guttatus (Kolis et al. 2022) to the larger genomes of M. cardinalis and M. parishii holds promise for mapping and population genomics across Mimulus. The mapped RILs are now a permanent resource for research on adaptation and speciation, particularly the study of fitness-relevant traits that benefit from the replication of recombinant genotypes under different biotic or abiotic conditions. Further, the extreme phenotypic diversity of these recombinant plants, their ease of culture, and the growing knowledge base of this flagship system make the RILs valuable for course-based undergraduate research experiences (CUREs) in genetics and evolution.

Overall, patterns of TRD, pseudolinkage, and hybrid sterility reveal substantial genic and chromosomal incompatibilities between this pair of naturally hybridizing taxa. Furthermore, with the exception of the Chromosome 6–7 translocation and consistent *M. cardinalis* excess in the YUP supergene region of Chromosome 4 (Liang et al. 2023), the specific loci and patterns of hybrid sterility and TRD appeared mostly idiosyncratic to this *M. parishii* × *M. cardinalis* cross, rather than shared with either

M. lewisii × M. cardinalis (Fishman et al. 2013) or M. parishii × M. lewisii hybrids (Fishman et al. 2015). Because hybrids between M. cardinalis and M. lewisii segregate for an additional translocation involving Chr 1 and Chr 8, severe underdominant pollen sterility likely overshadows other factors influencing the proportion of viable pollen (as each grain can only be sterile once) as well as patterns of marker TRD on Chromosome 8. However, we can conclude that at least 2 major postzygotic incompatibilities are not shared: the LG4-LG8 sexindependent gametophytic lethal detected here by TRD and LD (see more below) and the absent-here cytoplasmic male sterility (CMS) causing anther sterility and zero pollen production in a fraction of M. parishii x M. lewisii hybrids (Fishman et al. 2015). Here, the small-effect pollen number QTLs all have allelic effects consistent with M. parishii (also the organelle-donating grandparent, as in the M. parishii x M. lewisii CMS-producing cross) evolving lower pollen number as part of the selfing syndrome (Sicard and Lenhard 2011). In addition, although there is abundant and consistent TRD in M. parishii x M cardinalis hybrids, we did not recapitulate strong gametophytic TRD favoring M. cardinalis alleles on LG3 in M. lewisii x M. cardinalis hybrids (Fishman et al. 2013). In that cross, patterns of TRD in additional backcrosses revealed the mechanism to be singlelocus and strictly male-gametophytic, suggesting a locus involved in the evolution of faster pollen tube growth in the longer-styled hummingbird-pollinated species (Fishman et al. 2013). The absence of a parallel pattern here, where the parental difference in pollen

Table 2. Male fertility QTL locations and effects in M. parishii × M. cardinalis UM-F₂ and RIL populations.

| Pop. | Trait | LG/Chrom | cM position (1.5 LOD) | Mb position (1.5 LOD) | r ² | а | d | Summary |
|----------------|------------------|----------|--------------------------|-----------------------|----------------|--------|--------|----------|
| F ₂ | Pollen viability | 2 | 67.02 (65.3–69.1) | 43.96 (43.28–45.27) | 0.076 | 0.022 | 0.111 | H+ |
| | , | 3 | 40.59 (39.23–47.66) | 13.84 (12.30–42.72) | 0.062 | -0.007 | 0.105 | H+ |
| | | 4 | 26.93 (16.91–33.22) | 7.65 (3.44–13.26) | 0.071 | -0.073 | -0.040 | P-, dom. |
| | | 6&7* | 92.88 (91.39–94.88) | 6_60.55 (59.99–60.55) | 0.315 | -0.027 | -0.231 | H- |
| | | | + 149.95 (148.58–150.15) | + 7_9.92 (6.73–10.10) | | | | |
| | Pollen count | 1 | 8.95 (7.3–12.59) | 1.42 (1.32–2.48) | 0.076 | -8044 | -6254 | P-, dom. |
| | | 3 | 54.64 (49.84–57.78) | 46.39 (43.46–47.12) | 0.061 | -6764 | 8769 | P-, rec. |
| | | 6&7 | 155.55 (141.9–159.28) | 7_15.10 (4.13–21.30) | 0.064 | 1863 | 13,059 | H + |
| RIL | Pollen count | 1 | 50.37 (38.29–58.30) | 8.29 (5.52–10.96) | 0.111 | -5819 | | P- |
| | | 6 | 45.88 (38.64–56.53) | 7.54 (4.83–11.24) | 0.374 | -6830 | | P- |

Additive effects (a) and dominances (d) are negative when the M. parishii allele has a lower value. The summary column indicates the overall pattern of inheritance from a comparison of 2a vs a + d (H+ and H− mean overdominance and underdominance, respectively, while P− means the PAR allele reduces the trait value, and dom. and rec. (if present) indicates the overall dominance or recessivity, respectively, of the PAR allele. For the translocation-associated pollen viability QTL (6&7*) with a split location, effects are given for the higher peak. Dominance was not calculated in the RIL QTL model, which excluded heterozygotes.

tube growth should (if anything) be accentuated by greater divergence in flower size and mating system, suggests that the previously reported M. cardinalis pollen growth advantage against M. lewisii was dependent on the stylar or genetic context. Similarly, novel strong TRD favoring M. parishii homozygotes on Chr5 in our RILs (vs the opposite pattern in F_2 hybrids and in M. $parishii \times M$. lewisii hybrids) suggests specific selection generated by either the greenhouse environment at UGA or the process of RIL formation. Further targeted comparisons of such barrier loci across generations, as well as among the hybrids of these 3 closely related Erythranthe taxa, hold great promise for peeling away the complex layers of genetic interactions that shape hybrid genomes and phenotypes.

Chromosomal translocations: a major and remarkably persistent cause of hybrid sterility

Consistent with previous coarse mapping in M. lewisii x M. cardinalis and newly available genomes (Fig. 1), our results demonstrate that M. cardinalis carries a unique and strongly underdominant reciprocal translocation relative to closely related taxa. Inversions and translocations were among the first posited mechanisms of postzygotic reproductive isolation, as they provide cytogenetically visible evidence of hybrid genomic incompatibility (Stebbins 1958; White 1968; Grant 1971; King 1993). Although empirical studies in plant hybrids often find species-polymorphic and speciesdiagnostic inversions without underdominant effects on fertility (Zhang et al. 2021), translocations have been consistently associated with severe underdominant sterility (Lai et al. 2005; Fishman et al. 2013). Because the underdominant effect of translocations is a direct effect of chromosomal pairing in heterozygotes (Stathos and Fishman 2014), their initial spread postmutation should be strongly opposed by selection (Lande 1984, 1985) and remains paradoxical. Notably, both hummingbird-pollinated M. cardinalis (Chr 6 and 7) and bee-pollinated M. lewisii (Chr 1 and 8) each have at least one derived reciprocal translocation, while selfer M. parishii carries no novel major rearrangements; thus, strong drift likely does not explain the origin of translocations in this system. Furthermore, this study shows that enforced selfing after hybridization does not eliminate this chromosomal incompatibility and its fitness effects. Thus, rather than quickly sorting to parental chromosomes, translocations may have complex and persistent effects on fertility, recombination, and introgression upon secondary contact between chromosomally divergent plants.

The M. cardinalis Chromosome 6–7 translocation generates complex (nonlinear) linkage relationships across much of both chromosomes in F_2 hybrids with M. parishii (Fig. 1), exhibits elevated heterozygosity near the breakpoints (Fig. 2), and causes

severe underdominant F2 pollen inviability (Fig. 4). Substantial excess heterozygosity was retained around the translocation breakpoints (Fig. 2), and while some translocation-heterozygous RILs appear to have escaped to compatible chromosomal configurations, many of them exhibited the low pollen viability of their F₂ ancestors. Importantly, variation among heterozygous RILs did not appear to reflect the segregation of unlinked modifiers (i.e. one or the other parental genotype substantially conferring enhanced LG6&7 heterozygote fertility by specifying alternate segregation). None of the epistatic interactions between LG6&7 and each other sterility locus had the property of mitigating or exacerbating its underdominant pollen viability effects (Supplementary Fig. 6). This contrasts with previous work in M. lewisii × M. cardinalis hybrids, where M. cardinalis alleles on LG2 specifically accentuated the underdominant effects of the M. cardinalis translocation (Fishman et al. 2013).

This result suggests that translocations may have surprisingly persistent effects on fertility (as well as extended effects on patterns of genomic diversity and introgression) when selfing follows hybridization between structurally divergent incipient species. Population genomics shows that M. parishii has recently captured a Southern Californian M. cardinalis chloroplast, as well as nuclear regions (Nelson, Stathos, et al. 2021), suggesting a history of hybridization involving initial F₁ formation with M. cardinalis as the seed parent and then recurrent backcrossing to M. parishii and/ or selfing (plus possibly selection for M. parishii-like phenotypes). Since the CE10 chromosomal structure appears widespread throughout the M. cardinalis range (Fishman et al. 2013), we would predict that this genomic region may exhibit elevated diversity and/or unusual patterns of introgression where M. parishii hybridizes naturally with its hummingbird-pollinated relative. This scenario contrasts with the sorting expected for a typical barrier locus and suggests that translocations may behave differently from inversions associated with ecological barriers during speciation and secondary contact, at least in self-compatible plant species. Now that the interchange breakpoints between these naturally hybridizing taxa have been genetically and physically localized, and such predictions are testable with dense sampling in areas of sympatry between M. cardinalis and structurally divergent species.

More broadly, the strong and persistent effects of the *M. cardinalis-M. parishii* reciprocal translocation on linkage disequilibrium, heterozygosity, and sterility suggest that such incompatible chromosomal rearrangements deserve more theoretical and empirical study. Although the initial spread and fixation of species-diagnostic translocations are puzzling without extreme drift or meiotic drive (Lande 1984, 1985), they are an empirically major cause of hybrid

breakdown in plants (Grant 1971). Nonetheless, inversions have garnered more focus recently as causes of adaptive differentiation and species barriers, though they are rarely direct causes of hybrid sterility in plants. In mammals, on the other hand, Robertsonian translocations (centric fission/fusions) are common even within species (Garagna et al. 2014), but do not singly cause the kind of underdominant sterility seen with this Mimulus partial-arm translocation. Now that long-read sequencing technologies make the assembly of neargapless chromosomes possible across a diversity of systems, revisiting the genomic and molecular causes of organismally distinct patterns of chromosomal evolution and their direct and indirect effects on speciation is newly feasible. Plant systems where diverse chromosomal rearrangements contribute to adaptation and speciation from population to genus-wide scales, such as Helianthus (sunflowers [Ostevik et al. 2020; Owens et al. 2023]) and Mimulus, provide a promising forum for such work.

A novel sex-independent gametophytic incompatibility

Patterns of TRD in both F2 hybrids and RILs indicate absolute nontransmission of both male and female gametes with both M. cardinalis alleles on Chr 8 and M. parishii alleles on Chr 4 (Fig. 2; Supplementary Tables 1 and 6). This extreme pattern of distortion is consistent with a two-locus sex-independent gametophytic incompatibility. In land plants, which have a life cycle with 2 multicellular stages (a.k.a. alternation of generations), incompatibilities may act in the haploid gametophyte or in the diploid sporophyte to cause sterility. Unlike in animal sperm or egg cells (Braun et al. 1989), a substantial proportion of the genome is haploid-expressed in plant gametophytes (Honys and Twell 2004; Wuest et al. 2010; Rutley and Twell 2015). Reflecting this expression activity, most hybrid sterility loci in rice are gametophytic (Ouyang and Zhang 2013), and genome-wide patterns of TRD in multiple F2 populations of Arabidopsis lyrata also seem to be caused by gametic incompatibilities (Leppälä et al. 2013). Abundant gametophytic incompatibilities in plants might be due to the relatively large mutational target of haploid-expressed genes, to rapid divergent evolution of gametophytic genes under efficient sex-specific selection (Gossmann et al. 2013, 2016) or other natural selection (Immler and Otto 2018; Beaudry et al. 2020), or simply to the greater opportunity for exposure of negative allelic interactions in haploid hybrid tissues (similar to hemizygosity as an explanation for Haldane's rule).

The sex independence of the new M. parishii-M. cardinalis incompatibility implies a shared molecular mechanism for the loss of both male and female gamete function—but what could that be? Meiotic and developmental programs resulting in embryo sacs (female) and pollen (male) occur in distinct sexual organs of the flower, and sex-specificity of hybrid sterility loci is predominant in taxa that have been systematically studied, such as rice (Myint and Koide 2022). Nevertheless, sex-independent incompatibility loci have been identified in tomato (Rick 1966), rice (Sano 1990; Koide, Onishi, et al. 2008), lettuce (Giesbers et al. 2018), and yellow monkeyflowers (Kerwin and Sweigart 2017). Because core cellular processes such as meiosis and mitosis are critical for gametogenesis in both sexes, many of the same genes are essential in both sexes (Drews and Yadegari 2002; Ma et al. 2021; Yu et al. 2022; Zhou et al. 2022). Thus, the breakdown of these processes in hybrids could cause sex-independent incompatibility. However, because the LG4-LG8 gametic incompatibility does not colocalize with QTLs for either pollen number or viability, it implies a nonmitotic or meiotic mechanism that does not induce pollen abortion or substantially impair pollen development (at least in a way that could be assessed by our starch stain for

viability). This contrasts with the hms1-hms2 system in yellow monkeyflowers (Kerwin and Sweigart 2017), which causes both sex-independent TRD and pollen sterility, but parallels a sexindependent, 2-locus gametophytic barrier between wild and cultivated lettuce(Giesbers et al. 2018). The lack of a pollen-staining effect in both this study and lettuce intriguingly suggests the involvement of genes required specifically for the functioning of mature male and female gametophytes (e.g. genes involved in both female gametogenesis and pollen tube growth/guidance) (Leszczuk et al. 2019; Chen et al. 2020). Like a lethal incompatibility causing albinism in some hybrids between yellow monkeyflowers M. nasutus and M. guttatus (Zuellig and Sweigart 2018), the completeness of gamete failure might suggest duplication and reciprocal deletion of a haploid-essential gene as a potential mechanism. While the completely nontransmitted region on Chromosome 8 contains ~1,000 genes flanking a putatively centromeric region of low recombination, the interacting locus on Chromosome 4 is ~1 Mb containing only 80 genes. Given that parallels to other gametic lethals suggest a finite pool of functional candidate genes, the genetic and molecular mechanisms are thus amenable to further dissection.

Conclusions

Overall, our results underline the magnitude, complexity, and diversity of postmating barriers (including postzygotic) that can evolve between closely related plant species. A novel 2-locus sexindependent gametic Dobzhansky-Muller incompatibility and a reciprocal translocation each profoundly affect patterns of transmission and linkage disequilibrium across entire chromosomes. The genic incompatibility completely eliminates gametes recombinant between the 2 involved loci, thus acting as a strong barrier that should shape natural hybridization for whole genomic regions. In contrast, the underdominant reciprocal translocation causes retention of heterozygosity despite enforced selfing, suggesting that it may not act as a typical barrier gene flow despite its major fertility costs. Understanding the mechanisms and origins of these major incompatibilities is key for reconstructing the process of speciation in this model system, as well as predicting patterns of gene flow in areas of contact. Additional regions of consistent F2 TRD amplified across generations to even more strongly skew RIL composition, providing indirect evidence of substantial postmating or postzygotic barriers not detectable from measures of hybrid fertility alone. Beyond illustrating the rapid buildup of multiple postzygotic barriers and providing essential context for investigating the striking floral and life history divergence between these taxa, this work raises new questions about the evolutionary origins of such strong postzygotic barriers and their effects in natural hybrid zones.

Data availability

Raw sequence data from F2 and RIL mapping populations have been archived on the NCBI Sequence Read Archive under PRJNA1003462 and PRJNA948041, respectively. The genotype and phenotype data for linkage, transmission ratio distortion, and QTL mapping are archived on Dryad (doi:10.5061/dryad. v6wwpzh1m).

Supplemental material available at GENETICS online.

Acknowledgments

We thank T. C. Nelson, K. Baesen, and A. Demaree for lab assistance and O. Moynahan of the UM ECOR plant growth facility, M. Moriarty, M. Opel, and C. Liu of the UConn Botanical Conservatory, and Mike Boyd and Greg Cousins of the UGA Plant Sciences Greenhouse for assistance with plant care. We are especially indebted to S. McCann for his help in generating the RILs.

Funding

This work was supported by National Science Foundation grants DEB-1457763 and OIA-1736249 to LF, DEB-1350935 to ALS, and IOS-1827645 to ALS and YWY.

Conflicts of interest

The authors declare no conflict of interest.

Literature cited

- Angert AL, Bradshaw HD, Schemske DW. Using experimental evolution to investigate geographic range limits in monkeyflowers. Evolution. 2008;62(10):2660-2675. doi:10.1111/j.1558-5646.2008. 00471.x.
- Beardsley P, Yen A, Olmstead RG. AFLP phylogeny of Mimulus section Erythranthe and the evolution of hummingbird pollination. Evolution. 2003;57(6):1397-1410. doi:10.1111/j.0014-3820.2003. tb00347.x.
- Beaudry FEG, Rifkin JL, Barrett SCH, Wright SI. Evolutionary genomics of plant gametophytic selection. Plant Commun. 2020;1(6): 100115. doi:10.1016/j.xplc.2020.100115.
- Bolger AM, Lohse M, Usadel B. Trimmomatic: a flexible trimmer for Illumina sequence data. Bioinformatics. 2014;30(15):2114-2120. doi:10.1093/bioinformatics/btu170.
- Bradshaw HD, Otto KG, Frewen BE, McKay JK, Schemske DW. Quantitative trait loci affecting differences in floral morphology between two species of monkeyflower (Mimulus). Genetics. 1998;149(1):367-382. doi:10.1093/genetics/149.1.367.
- Bradshaw HD, Schemske DW. Allele substitution at a flower colour locus produces a pollinator shift in monkeyflowers. Nature. 2003;426(6963):176-178. doi:10.1038/nature02106.
- Bradshaw HD, Wilbert SM, Otto KG, Schemske DW. Genetic mapping of floral traits associated with reproductive isolation in monkeyflowers (Mimulus). Nature. 1995;376(6543):762-765. doi:10.1038/ 376762a0.
- Braun RE, Behringer RR, Peschon JJ, Brinster RL, Palmiter RD. Genetically haploid spermatids are phenotypically diploid. Nature. 1989;337(6205):373-376. doi:10.1038/337373a0.
- Burnham CR. Chromosomal interchanges in plants. Bot Rev. 1956; 22(7):419-552. doi:10.2307/4353549? refreqid=search-gateway: 9fe607409d09d1d32b601994ec68caaf.
- Chen D, Wang Y, Zhang W, Li N, Dai B, Dai B, Xie F, Sun Y, Sun Mengxiang, Peng X. Gametophyte-specific DEAD-box RNA helicase 29 is required for functional maturation of male and female gametophytes in Arabidopsis. J Exp Bot. 2020;71(14):4083-4092. doi:10.1093/jxb/eraa190.
- Colomé-Tatché M, Johannes F. Signatures of Dobzhansky-Muller incompatibilities in the genomes of recombinant inbred lines. Genetics. 2016;202(2):825-841. doi:10.1534/genetics.115.179473.
- Coughlan JM, Matute DR. The importance of intrinsic postzygotic barriers throughout the speciation process. Philos Trans R Soc Lond B Biol Sci. 2020;375(1806):20190533. doi:10.1098/rstb.2019.0533.
- Coyne JA, Orr HA. Speciation. Sunderland (MA): Sinauer Associates, Inc; 2004.
- Danecek P, Auton A, Abecasis G, Albers CA, Banks E, DePristo MA, Handsaker RE, Lunter G, Marth GT, Sherry ST, et al. The variant

- call format and VCFtools. Bioinformatics. 2011;27(15):2156-2158. doi:10.1093/bioinformatics/btr330.
- Drews GN, Yadegari R. Development and function of the angiosperm female gametophyte. Annu Rev Genet. 2002;36(1):99-124. doi:10. 1146/annurev.genet.36.040102.131941.
- Fishman L, Aagaard JE, Tuthill JC. Toward the evolutionary genomics of gametophytic divergence: patterns of transmission ratio distortion in monkeyflower (Mimulus) hybrids reveal a complex genetic basis for conspecific pollen precedence. Evolution. 2008;62(12):2958-2970. doi:10.1111/j.1558-5646. 2008.00475.x.
- Fishman L, Beardsley P, Stathos A, Williams CF, Hill JP. The genetic architecture of traits associated with the evolution of selfpollination in Mimulus. New Phytol. 2015;205(2):907-917. doi:10. 1111/nph.13091.
- Fishman L, McIntosh M. Standard deviations: the biological bases of transmission ratio distortion. Annu Rev Genet. 2019;53(1): 347-372. doi:10.1146/annurev-genet-112618-043905.
- Fishman L, Saunders A. Centromere-associated female meiotic drive entails male fitness costs in monkeyflowers. Science. 2008; 322(5907):1559-1562. doi:10.1126/science.1161406.
- Fishman L, Stathos A, Beardsley P, Williams CF, Hill JP. Chromosomal rearrangements and the genetics of reproductive barriers in Mimulus (monkeyflowers). Evolution. 2013;67(9):2547-2560. doi: 10.1111/evo.12154.
- Fishman L, Sweigart AL. When two rights make a wrong: the evolutionary genetics of plant hybrid incompatibilities. Annu Rev Plant Biol. 2018;69(1):707-731. doi:10.1146/annurev-arplant-042817-040113.
- Garagna S, Page J, Fernandez-Donoso R, Zuccotti M, Searle JB. The Robertsonian phenomenon in the house mouse: mutation, meiosis and speciation. Chromosoma. 2014;123(6):529-544. doi:10. 1007/s00412-014-0477-6.
- Giesbers AKJ, den Boer E, Ulen JJWEH, van Kaauwen MPW, Visser RGF, Niks RE, Jeuken MJW. Patterns of transmission ratio distortion in interspecific lettuce hybrids reveal a sex-independent gametophytic barrier. Genetics. 2018;211(1):263-276. doi:10. 1534/genetics.118.301566.
- Golczyk H, Massouh A, Greiner S. Translocations of chromosome end-segments and facultative heterochromatin promote meiotic ring formation in evening primroses. Plant Cell. 2014;26(3): 1280-1293. doi:10.1105/tpc.114.122655.
- Gossmann TI, Saleh D, Schmid MW, Spence MA, Schmid KJ. Transcriptomes of plant gametophytes have a higher proportion of rapidly evolving and young genes than sporophytes. Mol Biol Evol. 2016;33(7):1669-1678. doi:10.1093/molbev/msw044.
- Gossmann TI, Schmid MW, Schmid KJ. Selection-driven evolution of sexbiased genes is consistent with sexual selection in Arabidopsis thaliana. Mol Biol Evol. 2013;31(3):574-583. doi:10.1093/molbev/mst226.
- Grant V. Plant Speciation. New York (NY): Columbia University Press;
- Hiesey W, Nobs M, Bjorkman O. Experimental studies on the nature of species V. Biosystematics, Genetics and Physiological Ecology of the Erythranthe Section of Mimulus. Washington (DC): Carnegie
- Honys D, Twell D. Transcriptome analysis of haploid male gametophyte development in Arabidopsis. Genome Biol. 2004;5(11):R85. doi:10.1186/gb-2004-5-11-r85.
- Huang K, Rieseberg LH. Frequency, origins, and evolutionary role of chromosomal inversions in plants. Front Plant Sci. 2020;11:296. doi:10.3389/fpls.2020.00296.
- Immler S, Otto SP. The evolutionary consequences of selection at the haploid gametic stage. Am Nat. 2018;192(2):241-249. doi:10.1086/ 698483

- Kerwin RE, Sweigart AL. Mechanisms of transmission ratio distortion at hybrid sterility loci within and between Mimulus species. G3 (Bethesda). 2017;3(7):3719-3730. doi:10.1534/g3.117.300148.
- King M. Species Evolution: The Role of Chromosome Change. Cambridge: Cambridge University Press: 1993.
- Koide Y, Ikenaga M, Sawamura N, Nishimoto D, Matsubara K, Onishi K, Kanazawa A, Sano Y. The evolution of sex-independent transmission ratio distortion involving multiple allelic interactions at a single locus in rice. Genetics. 2008;180(1):409-420. doi:10.1534/ genetics.108.090126.
- Koide Y, Onishi K, Nishimoto D, Baruah AR, Kanazawa A, Sano Y. Sex-independent transmission ratio distortion system responsible for reproductive barriers between Asian and African rice species. New Phytol. 2008;179(3):888-900. doi:10.1111/j.1469-8137.2008.02490.x.
- Kolis KM, Berg CS, Nelson TC, Fishman L. Population genomic consequences of life-history and mating system adaptation to a geothermal soil mosaic in yellow monkeyflowers. Evolution. 2022; 76(4):765-781. doi:10.1111/evo.14469.
- Lai Z, Nakazato T, Salmaso M, Burke JM, Tang S, Knapp SJ, Rieseberg LH. Extensive chromosomal repatterning and the evolution of sterility barriers in hybrid sunflower species. Genetics. 2005; 171(1):291-303. doi:10.1534/genetics.105.042242.
- Lande R. The expected fixation rate of chromosomal inversions. Evolution. 1984;38(4):743. doi:10.2307/2408386.
- Lande R. The fixation of chromosomal rearrangements in a subdivided population with local extinction and colonization. Heredity (Edinb). 1985;54(3):323-332. doi:10.1038/hdy.1985.43.
- Leppälä J, Bechsgaard JS, Schierup MH, Savolainen O. Transmission ratio distortion in Arabidopsis lyrata: effects of population divergence and the S-locus. Heredity (Edinb). 2008;100(1):71-78. doi:10. 1038/sj.hdy.6801066.
- Leppälä J, Bokma F, Savolainen O. Investigating incipient speciation in Arabidopsis lyrata from patterns of transmission ratio distortion. Genetics. 2013;194(3):697-708. doi:10.1534/genetics.113. 152561.
- Leszczuk A, Szczuka E, Zdunek A. Arabinogalactan proteins: distribution during the development of male and female gametophytes. Plant Physiol Bioch. 2019;135:9-18. doi:10.1016/j.plaphy. 2018.11.023.
- Li H, Handsaker B, Wysoker A, Fennell T, Ruan J, Homer N, Marth G, Abecasis G, Durbin R, 1000 Genome Project Data Processing Subgroup, et al. The sequence alignment/map format and SAMtools. Bioinformatics. 2009;25(16):2078-2079. doi:10.1093/ bioinformatics/btp352.
- Liang M, Chen W, Lafountain AM, Liu Y, Peng F, Xia R, Bradshaw HD, Yuan Y-W. Taxon-specific, phased siRNAs underlie a speciation locus in monkeyflowers. Science. 2023;379(6632):576-582. doi: 10.1126/science.adf1323.
- Liang M, Foster CE, Yuan Y-W. Lost in translation: molecular basis of reduced flower coloration in a self-pollinated monkeyflower (Mimulus) species. Sci Adv. 2022;8(37):eabo1113. doi:10.1126/ sciadv.abo1113.
- Livingstone K, Churchill GA, Jahn MK. Linkage mapping in populations with karyotypic rearrangements. J Hered. 2000;91(6): 423-428. doi:10.1093/jhered/91.6.423.
- Livingstone K, Rieseberg LH. Chromosomal evolution and speciation: a recombination-based approach. New Phytol. 2004;161(1): 107-112. doi:10.1046/j.1469-8137.2003.00942.x.
- Ma T, Li E, Li L, Li S, Zhang Y. The Arabidopsis R-SNARE protein YKT61 is essential for gametophyte development. J Integr Plant Biol. 2021;63(4):676–694. doi:10.1111/jipb.13017.

- Matute DR, Comeault AA, Earley E, Serrato-Capuchina A, Peede D, Monroy-Eklund A, Huang W, Jones CD, Mackay TFC, Coyne JA. Rapid and predictable evolution of admixed populations between two Drosophila species pairs. Genetics. 2020;214(1):211-230. doi: 10.1534/genetics.119.302685.
- McKenna A, Hanna M, Banks E, Sivachenko A, Cibulskis K, Kernytsky A, Garimella K, Altshuler D, Gabriel S, Daly M, et al. The genome analysis toolkit: a MapReduce framework for analyzing nextgeneration DNA sequencing data. Genome Res. 2010;20(9): 1297-1303. doi:10.1101/gr.107524.110.
- Moyle LC, Nakazato T. Comparative genetics of hybrid incompatibility: sterility in two Solanum species crosses. Genetics. 2008; 179(3):1437-1453. doi:10.1534/genetics.107.083618.
- Myint ZM, Koide Y. Influence of gender bias on distribution of hybrid sterility in rice. Front Plant Sci. 2022;13:898206. doi:10.3389/fpls. 2022.898206.
- Nelson TC, Muir CD, Stathos AM, Vanderpool DD, Anderson K, Angert AL, Fishman L. Quantitative trait locus mapping reveals an independent genetic basis for joint divergence in leaf function, life-history, and floral traits between scarlet monkeyflower (Mimulus cardinalis) populations. Am J Bot. 2021;108(5):844-856. doi:10.1002/ajb2.1660.
- Nelson TC, Stathos AM, Vanderpool DD, Finseth FR, Yuan Y-W, Fishman L. Ancient and recent introgression shape the evolutionary history of pollinator adaptation and speciation in a model monkeyflower radiation (Mimulus section Erythranthe). PLoS Genet. 2021;17(2):e1009095. doi:10.1371/journal.pgen.1009095.
- Noor MAF, Grams KL, Bertucci LA, Reiland J. Chromosomal inversions and the reproductive isolation of species. Proc Natl Acad Sci U S A. 2001;98(21):12084-12088. doi:10.1073/pnas.221274498.
- Ostevik KL, Samuk K, Rieseberg LH. Ancestral reconstruction of karyotypes reveals an exceptional rate of nonrandom chromosomal evolution in sunflower. Genetics. 2020;214(4):1031-1045. doi:10. 1534/genetics.120.303026.
- Ouyang Y, Zhang Q. Understanding reproductive isolation based on the rice model. Annu Rev Plant Biol. 2013;64(1):111-135. doi:10. 1146/annurev-arplant-050312-120205.
- Owens GL, Huang K, Todesco M, Rieseberg LH. Re-evaluating homoploid reticulate evolution in Helianthus sunflowers. Mol Biol Evol. 2023;40(2):msad013. doi:10.1093/molbev/msad013.
- Paradis E. Pegas: an R package for population genetics with an integrated-modular approach. Bioinformatics. 2010;26(3):419-420. doi:10.1093/bioinformatics/btp696.
- Pritchard VL, Edmands S. The genomic trajectory of hybrid swarms: outcomes of repeated crosses between populations of Tigriopus californicus. Evolution. 2012;67(3):774-791. doi:10.1111/j.1558-5646.2012.01814.x.
- Ramsey J, Bradshaw HD, Schemske DW. Components of reproductive isolation between the monkeyflowers Mimulus lewisii and M. cardinalis (Phrymaceae). Evolution. 2003;57(7):1520-1534. doi:10. 1111/j.0014-3820.2003.tb00360.x.
- Rastas P. Lep-MAP3: robust linkage mapping even for low-coverage whole genome sequencing data. Bioinformatics. 2017;33(23): 3726-3732. doi:10.1093/bioinformatics/btx494.
- R Core Team. R: A Language and Environment for Statistical Computing. Vienna, Austria: Foundation for Statistical Computing; 2021. https://www.R-project.org/.
- Rick CM. Abortion of male and female gametes in the tomato determined by allelic interaction. Genetics. 1966;53(1):85-96. doi:10. 1093/genetics/53.1.85.
- Rieseberg LH. Chromosomal rearrangements and speciation. Trends Ecol Evol. 2001;16(7):351–358. doi:10.1016/s0169-5347(01)02187-5.

- Rutley N, Twell D. A decade of pollen transcriptomics. Plant Reprod. 2015;28(2):73–89. doi:10.1007/s00497-015-0261-7.
- Sano Y. The genic nature of gamete eliminator in rice. Genetics. 1990; 125(1):183–191. doi:10.2307/23785264? ref=search-gateway: 09c4fb7f0eff48940e08de7a2501c94d.
- Schemske DW, Bradshaw HD. Pollinator preference and the evolution of floral traits in monkeyflowers (Mimulus). Proc Natl Acad Sci U S A. 1999;96(21):11910–11915. doi:10.1073/pnas.96.21.11910.
- Sicard A, Lenhard M. The selfing syndrome: a model for studying the genetic and evolutionary basis of morphological adaptation in plants. Ann Bot. 2011;107(9):1433–1443. doi:10.1093/aob/mcr023.
- Stathos A, Fishman L. Chromosomal rearrangements directly cause underdominant F1 pollen sterility in Mimulus lewisii–Mimulus cardinalis hybrids. Evolution. 2014;68(11):3109–3119. doi:10.1111/evo.12503.
- Stebbins GL. The inviability, weakness, and sterility of interspecific hybrids. Adv Genet. 1958;9:147–215. doi:10.1016/s0065-2660(08) 60162-5.
- Thompson KA, Peichel CL, Rennison DJ, McGee MD, Albert AYK, Vines TH, Greenwood AK, Wark AR, Brandvain Y, Schumer M, et al. Analysis of ancestry heterozygosity suggests that hybrid incompatibilities in threespine stickleback are environment dependent. PLoS Biol. 2022;20(1):e3001469. doi:10.1371/journal.pbio.3001469.
- Wang S, Basten CJ, Zeng Z-B. Windows QTL Cartographer 2.5. Dept. of Statistics, North Carolina State University; 2005.
- Walter GM, Richards TJ, Wilkinson MJ, Blows MW, Aguirre JD, Ortiz-Barrientos D. Loss of ecologically important genetic variation in late generation hybrids reveals links between adaptation and speciation. Evol Lett. 2020;4(4):302–316. doi:10.1002/evl3.187.
- White MJD. Models of speciation. Science. 1968;159(3819):1065–1070. doi:10.1126/science.159.3819.1065.
- Wuest SE, Vijverberg K, Schmidt A, Weiss M, Gheyselinck J, Lohr M, Wellmer F, Rahnenführer J, von Mering C, Grossniklaus U, et al. Arabidopsis female gametophyte gene expression map reveals similarities between plant and animal gametes. Curr Biol. 2010; 20(6):506–512. doi:10.1016/j.cub.2010.01.051.

- Yin TM, DiFazio SP, Gunter LE, Riemenschneider D, Tuskan GA. Large-scale heterospecific segregation distortion in Populus revealed by a dense genetic map. Theor Appl Genet. 2004;109(3): 451–463. doi:10.1007/s00122-004-1653-5.
- Yu H, Zhang L, He X, Zhang T, Wang C, Lu J, He X, Chen K, Gu W, Cheng S, et al. OsPHS1 is required for both male and female gamete development in rice. Plant Sci. 2022;325:111480. doi:10.1016/j.plantsci.2022.111480.
- Yuan Y-W. Monkeyflowers (Mimulus): new model for plant developmental genetics and evo-devo. New Phytol. 2019;222(2):694–700. doi:10.1111/nph.15560.
- Yuan Y-W, Rebocho AB, Sagawa JM, Stanley LE, Bradshaw HD. Competition between anthocyanin and flavonol biosynthesis produces spatial pattern variation of floral pigments between Mimulus species. Proc Natl Acad Sci U S A. 2016;113(9): 2448–2453. doi:10.1073/pnas.1515294113.
- Zeng ZB. 1993. Theoretical basis for separation of multiple linked gene effects in mapping quantitative trait loci. Proc Natl Acad Sci. 90(23):10972–10976. doi:10.1073/pnas.90.23.10972
- Zeng ZB. 1994. Precision mapping of quantitative trait loci. Genetics 136(4):1457–1468. doi:10.1093/genetics/136.4.1457
- Zhang L, Reifová R, Halenková Z, Gompert Z. How important are structural variants for speciation? Genes (Basel). 2021;12(7): 1084. doi:10.3390/genes12071084.
- Zhou Y, Fang W, Pang Z, Chen L-Y, Cai H, Ain N-U, Chang M-C, Ming R. AP1G2 Affects mitotic cycles of female and male gametophytes in Arabidopsis. Front Plant Sci. 2022;13:924417. doi:10.3389/fpls. 2022.924417.
- Zuellig MP, Sweigart AL. Gene duplicates cause hybrid lethality between sympatric species of Mimulus. PLoS Genet. 2018;14(4): e1007130. doi:10.1371/journal.pgen.1007130.

Editor: L. Moyle